

CHAPTER 2

LITERATURE REVIEW

In 1996, Subramanian *et al.* [11] reviewed the mechanisms of wear and degradation in several manufacturing scenarios and considered the available published correlations between wear resistance and microstructure, hardness, toughness and adhesion of coatings. Based on the knowledge of strengthening mechanism in bulk materials, various possible ways to strengthen and improve coatings were discussed.

Noda *et al.* [5] reported on the plasma carburization of Ti-33.5Al-1Nb-0.5Cr-0.5Si (mass%) on fully lamellar cast alloy. The induced surface layer, 3 μm thickness, was Ti_2AlC with a hardness that was higher than a bearing steel AISI52100. The pin-on-disk test showed that the carburized pin possessed excellent wear resistance against the steel disk. The carburization did not cause deterioration of the tensile and fatigue properties at room temperature. The plasma carburization could improve the wear resistance of the TiAl.

Tian and Nemoto [8] reported the effect of carbon addition on the microstructures and mechanical properties of TiAl intermetallic alloys. It was shown that carbon is an efficient solid solution strengthener in TiAl and an efficient precipitation strengthener by fine dispersion of carbide. Transmission electron microscope observation revealed that fine needle-like precipitates, which lie only in one direction parallel to the (001) axis, appear in carbon doped TiAl during aging at temperature around 1073 K after quenching from 1523 K. Selected area electron diffraction analysis had shown that the needle-shaped precipitated was perovskite type, Ti_3AlC (P-phase). The orientation relationship between the P-phase and the TiAl matrix was found to be $(001)_\text{P} // (001)_{\text{TiAl}}$ and $(010)_\text{P} // (010)_{\text{TiAl}}$. By aging higher temperatures or for longer periods at 1073 K, plate-like precipitates of Ti_2AlC (H-phase) with a hexagonal crystal structure are formed on the {111} planes of TiAl matrix. TiAl doped with carbon was hardened appreciably by the fine precipitation of carbide. The deviation from the stoichiometry has a significant effect on the aging

behavior of TiAl. High temperature strength of TiAl increased appreciably by the precipitation of fine carbide. Dislocations bypass the carbide needles at further higher temperatures. The calculation of Orowan stress showed a good agreement with the experimental result.

In 1997, Guu *et al.* [12] reviewed the tribological behaviors of TiN, TiC and Ti(C,N) coatings prepared by differing mass flow rates of nitrogen and acetylene during the coating process. The specimens were coated with titanium film as the underlayer and with TiN, TiC or Ti(C,N) film as the top layer. They were deposited by the cathodic arc ion plating process. The chemical compositions of the ceramic coating were determined by the wavelength-dispersive x-ray analysis. The influence of mass flow rate ratio of N_2 and C_2H_2 gases on the tribological behavior, microhardness, coating morphology and adhesive strength was investigated. The three-body abrasive wear appears more often at the temperature that the ceramic coating was not yet softened by the frictional heat. Increasing the mass flow rate ratio of the acetylene gas in the coating process was favorable for more ions to react with titanium resulting in noticeable rising of the C/Ti atomic ratio. Conversely, it was disadvantageous for nitrogen ions to react with titanium. The wear rate of the specimen with the TiN film was the lowest but its friction coefficient was relatively higher than that of the TiC film.

In 1998, Thongtem *et al.* [7] reported the effect of gas nitridation of TiAl alloys on wear resistance. γ -TiAl alloys had been treated in ammonia gas for 100 h at temperatures between 1000 K and 1200 K to form TiN surface layers. The nitrided layers had been characterized by x-ray diffraction, microhardness measurements and a pin-on-disk apparatus. The friction coefficient was reduced substantially by the nitridation treatment. The wear rate of the nitrided alloys was reduced by two or three orders of magnitude in comparison with the untreated alloys. The effects increased with increasing treatment temperature over the temperature range studied.

Voltz *et al.* [21] reported on structural investigations of TiN films formed by covering a thermal vapor deposited titanium film on silicon (100) using nitrogen plasma immersion ion implantation. The nitrogen ions were implanted by applying high-voltage pulses of -45 kV amplitude in a nitrogen plasma generated by microwave excitation in the electron cyclotron resonance mode. Phase formation was

investigated by x-ray diffraction (XRD) and electron diffraction. The morphology of the films depending on the pulse number was determined by cross-sectional transmission electron microscopy (XTEM). With increasing pulse number, corresponding to an increasing implantation dose, TiN peaks appeared in XRD spectra, whereas the metal peaks became smaller and finally disappeared. XTEM results showed that Ti layer was radiation-damaged at the Ti/Si interface when the pulse number is small. Increasing the dose is the result to the formation of fine crystalline with slightly elongated TiN grains. For the highest doses, amorphous zones in the Si bulk as well as nanocrystalline TiN regions were observed.

In 2000, Musil and Hruby [16] reviewed $Ti_{1-x}Al_xN$ films prepared by magnetron sputtering. $Ti_{1-x}Al_xN$ films were sputtered on TiAl (60/40 at.%) target in Ar and Ar + N_2 mixture at a constant total pressure of 0.5 Pa. Films were sputtered at different pressures of nitrogen (p_{N_2}) ranging from 0 to 0.2 Pa. Different substrate temperature ranging from room temperature to 400 °C and two substrates biased at -200 V were used. It was found that the continuous change in p_{N_2} induced a dramatic change in the film structure and different values of microhardness of $Ti_{1-x}Al_xN$ films produced at different p_{N_2} which correlated very well with change in the film structure. Superhard films with hardness of up to 47 GPa were prepared. The superhard films were TiAl/AlN nanocomposite films composed of relatively large TiAlN grains (~ 30 nm), oriented in one direction and surrounded by an amorphous and/or nano-composite AlN phase. These films exhibited a high elastic recovery up to 74% and contained about 20 at% Al and 55 at% N.

Onuma et al. [10] presented the phase equilibria between the β -Ti, α -Ti, α_2 -Ti₃Al and the γ -TiAl in the Ti-Al system using specimens with low levels of oxygen as shown in Figure 2.1. The results obtained on the α/γ and the α_2/γ equilibria were in good agreement with the previous experiment and calculated phase boundaries, while the ones obtained on the α/β equilibrium deviated significantly from the previously proposed phase diagram. The β phase field extended to higher aluminum contents and the width of the $\alpha + \beta$ two-phase region was very narrow which is less than 1 at.% Al. The presence of the β -Ti/ β_2 -TiAl order/disorder transition in the β phase was also confirmed by a combination of differential scanning calorimetric (DSC) analysis and

extrapolation of ordering phase boundaries from the Ti-Al-X (X = Cr, Fe) ternary systems. A thermodynamic analysis had been carried out taking into account the ordering configuration in the β -Ti/ β_2 -TiAl, f.c.c.-Al/ γ -TiAl and α -Ti/ α_2 -Ti₃Al equilibria. It was proposed that the anomalous α/β equilibrium was due to the β -Ti/ β_2 -TiAl ordering reaction.

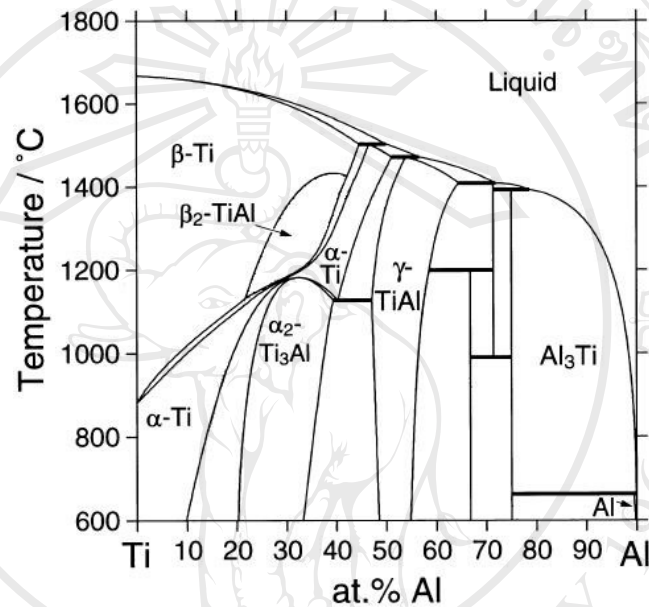


Figure 2.1 Ti-Al phase diagram.

Kainuma *et al.* [9] reported the phase equilibria between the α , α_2 , β and the γ phases in the Ti-Al base ternary systems investigated over the temperature range 1000 - 1300 °C. The tie lines and the phase boundaries were determined by electron probe microanalysis using multiphase alloys. It was showed that almost all the elements except Zr tended to partition into the β phase rather than into the α , α_2 , or γ phase, while Zr mostly partitioned into the γ phase. At 1000 °C, the equilibrium state between the α_2 and γ phases, V, Cr, Mo, Ta and W partitioned to the α_2 phase rather than to the γ phase, whereas Mn, Fe, Co, Ni, Cu and Zr tended to concentrate into the γ phase. The partition coefficients for the alloying elements were only slightly dependent on their concentrations.

In 2001, Wei *et al.* [13] reported on the coating sequence and coating thickness of titanium nitride and titanium carbonitride films on S45C steel substrate as

the top and the second layers of a multilayer system. These arrangements were made in order to investigate the mechanical properties of the composite films like the adhesion strength, load carrying capacity, hardness, surface morphology and surface microstructure. The experimental result showed that the specimens with the Ti/TiCN/TiN film have a relatively higher composite hardness than the Ti/TiN/TiCN film. The trend exhibited in the coating film hardness of ceramic coating film was similar to the composite hardness. The specimens with the Ti/TiCN/TiN film have a lower critical friction force and critical track distance comparing to the Ti/TiN/Ti(C,N) film. For the specimen with the Ti/TiCN/TiN film peaks protruding over the flat surface is quantitatively increased by the increase in the coating film thickness. Either the peak roughness (R_z) or the amplitude roughness (R_y) after coating thick films was strongly affected by the average roughness (R_a) of steel substrate before coating. The uniformity of the surface morphology can thus be improved. For the specimen with the Ti/TiN/TiCN film, increasing the total film thickness decreased the asperity and the morphological uniformity.

Wei *et al.* [14] reviewed the effect on the tribological behavior of the lower specimen disc with different total film thickness and different coating sequences of TiN and TiCN films. The tribological behavior in response to the above two factors was expressed in terms of the wear rate of the upper and lower specimen, friction coefficient, wear mechanism, wear debris size and wear displacement. The lower specimen wear rates could be regressed by two straight lines or two curves as a function of the friction power parameter. Friction coefficients could be expressed as two linear functions in terms of the parameter T/LV , where T , L and V are the specimen's ultimate temperature, applied load and the sliding velocity, respectively. The characteristics exhibited in the wear rate of the lower specimen and friction coefficient in each sub-region of the friction power parameter (fLV , where f is the average friction coefficient of entire wear process) and the parameter T/LV , respectively could be interpreted by the alteration in wear mechanism. The wear rate of the lower specimen for TiCN film on the top layer is equivalent to or lower than that for TiN film on the top layer if they were both evaluated at the same thickness and operating conditions.

Shieh and Hon [17] reviewed the investigation on nanostructure and hardness of TiAlN thin film with different compositions prepared by plasma enhanced chemical vapor deposition. The deposited phase and microstructure of $Ti_{1-x}Al_xN$ were characterized by x-ray diffraction, scanning electron microscopy and transmission electron microscopy. Film hardness and reduced elastic modulus were measured by nanoindentation interfaced with an atomic force microscope. High-resolution transmission electron micrographs showed that grain size of $Ti_{1-x}Al_xN$ is decreased to less than 10 nm with the increasing of aluminium contents up to a ratio of $Al/(Al+Ti) = 0.63$. Hardness measurement showed that the microstructure feature was the most important factor in determining the hardness value of the films.

Kawata *et al.* [18] presented the characterization of TiAlN films deposited by pulsed d.c. plasma-enhanced chemical vapor deposition (PECVD). $Ti_{0.58}Al_{0.42}N$ (upper)/TiN(lower) double-layered films were prepared on steel substrates by pulsed d.c. PECVD at 823 K using gas mixtures of $TiCl_4$, $AlCl_3$, N_2 , H_2 and Ar. Glow discharge optical emission spectroscopy analysis revealed that chlorine concentration was much lower in the upper-layered film than in the TiN layer but with the same NaCl structure. The double-layered films had high oxidation resistance, a low friction coefficient and high wear resistance. The double-layered films demonstrated the superior soldering and corrosion resistance in a molten aluminium alloy at 953 K.

Kawata *et al.* [19] presented TiAlN/TiN, TiAlCN/TiAlN/TiN and TiAlON/TiAlN/TiN multilayer films which were prepared on steel substrates by pulsed d.c. plasma-enhanced chemical vapor deposition (PECVD) at 823 K using gas mixtures of $TiCl_4$, $AlCl_3$, N_2 , H_2 , CH_4 , O_2 and Ar. Fracture cross-sections of the TiAlN and TiAlCN films showed columnar structure. The TiAlON films are amorphous-like dense structure. XRD analysis showed that the TiAlN, TiAlCN and TiAlON films had NaCl structure. The XRD peaks of the TiAlON films were broad. Glow discharge optical emission spectroscopy analysis proved that these films are multilayer structure. Vickers hardness of the TiAlN/TiN, TiAlCN/TiAlN/TiN and TiAlON/TiAlN/TiN multilayer films were 2608, 2815 and 1444 HV, respectively. These multilayer films had higher oxidation resistance and better tribological properties than the TiN single-layer films. The TiAlCN/TiAlN/TiN multilayer films

showed the best wear resistance. Furthermore, these multiplayer films demonstrated superior corrosion resistance in a molten aluminium alloy at 953 K. The TiAlON/TiAlN/TiN multiplayer films indicated the best corrosion resistance.

Perdrix *et al.* [26] reviewed carbon effects on microstructural and mechanical properties of Ti-48Al fully lamellar alloy. The carbon concentrations were increased from 20 to 6000 wt. ppm. The lamellar structure was obtained for alloys slowly cooled ($35\text{ }^{\circ}\text{C}\cdot\text{min}^{-1}$) from 1350 $^{\circ}\text{C}$. Carbon in solid solution increased lattice parameters of the α_2 phase. In their study, the solubility limit of carbon is 3000 wt. ppm. For higher carbon contents, Ti_2AlC precipitates in the γ phase, leading to grain size decrease. Carbon in solid solution is the element to increase the α_2 volume fraction, microhardness, yield stress but to decrease the minimum creep rate. Precipitation of the Ti_2AlC did not modify these parameters except yield stress which is further increased. Comparison was made with previous results obtained from alloys with similar contents of either oxygen or nitrogen. Emphasis was put on the importance of a phase hardening by solute interstitial elements on the mechanical properties of lamellar alloy.

In 2002, Matsuura and Kudoh [25] reviewed surface modification of titanium by a diffusional carbonitridation. Titanium specimens were heated at temperatures between 1388 and 1573 K in graphite cup in an atmosphere of pure nitrogen, all the surfaces of the specimen were covered with a layer of titanium monocarbonitride (TiCN) and the layer of nitrogen-rich α -Ti had formed under the TiCN layer. The thicknesses of those layers are increased with the increase in both temperature and time in accordance with the parabolic law. By using Arrhenius' equation, the parabolic rate constants or diffusivity for the increased in thicknesses of the layers of the TiCN and α -Ti were described by the equations, $D_1 = 4.28 \times 10^{-5} \exp(-217000/RT)$ and $D_2 = 1.86 \times 10^{-5} \exp(-119000/RT) \text{ m}^2 \cdot \text{s}^{-1}$, respectively. Vickers hardness of the TiCN layer remained at approximately $2000 \text{ kg}\cdot\text{mm}^{-2}$ but that of the α -Ti layer gradually decreased from 1500 to $500 \text{ kg}\cdot\text{mm}^{-2}$, deep into the surface. The carbonitrided titanium exhibited high bending strength and excellent resistances in wear and corrosion comparing to those of pure titanium.

Zhao *et al.* [6] reported on gas nitridation of TiAl based alloys in ammonia. It was found that an Al-rich region formed below the nitride/sublayer interface. After nitridation, TiN, Ti₂AlN, Ti₃N_{2-x}, Ti₂N and Al-rich intermetallic phase (Ti₂Al₅) were detected. The total depth of the nitrided layers is increased with the increasing nitridation time and temperature. In comparison with non-nitrided alloy, the Knoop hardness of the nitrided alloys was higher. The hardness value of the alloy nitrided at 1213 K for 50 h was the maximum at 1629 kg.mm⁻².

Carrasco *et al.* [15] presented the determination of the residual macroscopic stresses in TiN coatings deposited by DC planar magnetron sputtering (DCPMS) on a Cu-3Ti-1Cr alloy under different conditions of applied current intensity, Ar/N₂ flow ratio and bias voltage. The residual stresses were measured by XRD with a grazing technique for films of 1 μm thick. These stresses were mainly due to the intrinsic stress. The total stresses have a small contribution of thermal stress, which was not important at the process temperature, in comparison with intrinsic stress. The state of the residual stresses controlled by the process parameters during deposition. These results were analysed with respect to the measures obtained for lattice parameter free of deformation, grain size, adhesion of the coat on the substrate, microhardness and chemical composition of the coating, in order to relate the stress evolution with these process parameters.

In 2003, Huber *et al.* [23] reviewed the formation of TiN, TiC and TiCN by metal plasma immersion ion implantation and deposition. With a titanium cathode and both nitrogen and methane gases, a series of compound TiC_xN_y could be prepared with the final points TiN and TiC using metal plasma immersion ion implantation and deposition. The respective properties of the films were investigated by XRD and Rutherford backscattering spectroscopy. With increasing pulse voltage, a decreasing carbon content and growth rate was found for the TiC series, while no such effect was observed for the corresponding TiN films.

In 2004, Fouquet *et al.* [20] reported the characterization of Ti-6Al-4V nitrided in radio-frequency (RF) plasma equipment using a N₂-H₂ gas mixture under 10 Pa with 30 - 720 min nitriding time and 500 - 900 °C nitriding temperature. In order to evidence the plasma efficiency, thermal treatment of nitridation, assisted or not by RF plasma, were performed in the same condition. The nitrided specimen were

characterized using XRD, SEM, TEM, EELS and microhardness tester. The plasma was shown to enhance the formation of richer compounds like δ -TiN and ε -Ti₂N nitrides on the surface at lower temperature than that obtained with a classic thermal treatment. This led to a significant reduction of the residual compressive stress. At 700 °C and for longer treatments, the plasma treatment enabled the formation of a TiN layer which was thought to act as a diffusion barrier for nitrogen. Then, the underneath previously formed Ti₂N grains underwent a nitrogen rearrangement with the remaining α -Ti grains leading to the formation of a nonstoichiometric phase that was identified as the TiN_{0.26}.

Tang *et al.* [22] presented the synthesis of TiC films by plasma immersion ion implantation and deposition on AISI440B bearing steel. Acetylene plasma was produced by RF plasma source, and titanium plasma was generated by cathodic arc plasma source. Influences of gas pressure and pulse width of the bias voltage on properties of the thin film were investigated. The as-deposited films were characterized by XRD, microhardness tester, pin-on-disk apparatus and electrochemistry corrosion equipment. XRD pattern proved that TiC phase formed in the film. Comparing to the uncoated substrates, the maximum micro-hardness was increased by 70.8%. In addition, the friction coefficient was decreased to about 0.1, and the corrosion resistance of the coated substrate surfaces was improved significantly.

Sen [24] reviewed the growth kinetics of TiN layer deposited on pre-nitrided AISI 1020 steel samples by thermo-reactive diffusion (TRD) technique in a solid medium. Steel was firstly tufftrided and TiN coating treatment was performed in a powder mixture consisting of ferro-titanium, ammonium chloride and alumina at 1173, 1223 and 1273 K for 1 – 4 h. TiN layer on the titanium nitride coated AISI 1020 steel ranging from 5.5 to 19.2 μm depending on the treatment time and temperature. The depth of TiN layer was characterized as a function of time and temperature and fitted to the Arrhenius type equation. It shows that the diffusion coefficient (D) of the process is increased with the treatment temperature. Calculated activation energy for TRD process is 187.09 $\text{kJ}\cdot\text{mol}^{-1}$. The D is varied between 6.637×10^{-11} and 2.097×10^{-10} $\text{cm}^2\cdot\text{s}^{-1}$ depending on the process temperature.